AD-A995 126

UNCLASSIFIED

CONFIDENTIAL SECURITY INFORMATION

Per DA2A
93172
dtd 8 Aug 60

DDESB Library Copy

AFSWP-460

USADAC TECHNICAL LIBRARY
5 0712 01021047 3

ON THE EFFECT OF SLOW RISE TIMES ON THE BLAST LOADING OF STRUCTURES

M. L. Merritt, 5111

September 25, 1953

UNCLASSIFIED

RESTRICTED DATA

This document contains restricted data as defined in the Atomic Energy Act of 1946. Its transmittal or the disclosure of its contents in any manner to an unauthorized person is prohibited.

This document consists of 38 pages
No. 236 of 266 copies, series A

Sandia Corporation
CONTRACTORS FOR U.S. ATOMIC ENERGY COMMISSION
ALBUQUERQUE • NEW MEXICO

CONFIDENTIAL SECURITY INFORMATION

20

UNCLASSIFIED

7

ABSTRACT

In an enquiry into the effects of precursor-type and other nonideal blast waves on the loading of structures, attention is fixed on the effects of slow rise times. This is approached through the medium of sound-pulse theory, and there is derived a very simple rule for accounting for their effects. It is then argued that this rule, exact in the acoustic case, is approximately correct for shocks of finite strength.

In the course of the argument a calculation is made of loading on a structure for a step-function incident wave. This result is compared with shock-tube results and various standard estimates of loading.

Finally, it is pointed out that consideration of slow rise times touches on but part of a larger problem.

PHOTOGRAPH THIS SHEET

AD A095126

DTIC ACCESSION NUMBER

LEVEL

INVENTORY

On the Effect of Slow Rise Times on the Blast Loading of Structures

DOCUMENT IDENTIFICATION

25 Sept. 53

Rept. No. AFSWP-460

DISTRIBUTION STATEMENT A

Approved for public release;
Distribution Unlimited

DISTRIBUTION STATEMENT

ACCESSION FOR		
NTIS	GRA&I	☒
DTIC	TAB	☐
UNANNOUNCED		☐
JUSTIFICATION		
(25 Sept. 1953)		
BY		
DISTRIBUTION /		
AVAILABILITY CODES		
DIST	AVAIL AND/OR SPECIAL	
A		

Released

DISTRIBUTION STAMP

DTIC
ELECTE
DEC 7 1981
S D
D

DATE ACCESSIONED

UNANNOUNCED

81 12 02 013

DATE RECEIVED IN DTIC

PHOTOGRAPH THIS SHEET AND RETURN TO DTIC-DDA-2

DTIC FORM OCT 79 70A

DOCUMENT PROCESSING SHEET

DISPOSITION FORM

For use of this form, see AR 340-15, the proponent agency is TAGCEN.

REFERENCE OR OFFICE SYMBOL	SUBJECT
TISI	Review of Document for Open Publication

TO TITL FROM TISI DATE 31 May 78 CMT 1

Reference your DF dated 28 April 1978 requesting review of the following document for open publication. The document has been cleared for open publication per the attached DF from ISCM.

AFWSP-460 "On The Effect of Slow Rise Times on the Blast Loading of Structures" - DTL-005,786

Theresa J. Egan

THERESA J. EGAN
Chief, Scientific Information Division

1 Incl
as

FORM 1 JAN 61 2496 REPLACES DD FORM 96, WHICH IS OBSOLETE.

CONFIDENTIAL

UNCLASSIFIED

TABLE OF CONTENTS

	Page
ABSTRACT	2
ON THE EFFECT OF SLOW RISE TIMES ON THE BLAST LOADING OF STRUCTURES	
Statement of the Problem	5
The Sound-Pulse Theories	8
Application of the Theory	13
The Effects of a Slow Rise	20
Comparison with Previous Estimates	20
Applicability to Finite Shocks under Actual Conditions	27
Conclusions	30
LIST OF REFERENCES	32

UNCLASSIFIED

CONFIDENTIAL

LIST OF ILLUSTRATIONS

	Page
Fig. 1a -- Ideal shock wave	5
Fig. 1b -- Typical gauge record in the early precursor region	6
Fig. 1c -- Typical gauge record in the late precursor region	6
Fig. 2 -- Idealization of nonideal shock wave	7
Fig. 3 -- Interaction of a shock wave with a wedge	8
Fig. 4a -- Diffraction pressure corrections for top of wedge	11
Fig. 4b -- Diffraction pressure corrections for front and back of wedge	12
Fig. 5 -- Space-time plot of pressures on a 2:1 building	14
Fig. 6 -- Space-time plot of loading on a 2:1 building	16
Fig. 7 -- Pressure profiles of loading on a 2:1 building	17
Fig. 8 -- Forces on the front and top of a 2:1 building	18
Fig. 9 -- Correction of forces for a finite rise time, $ct_r = 0.4H$	21
Fig. 10 -- Correction of forces for a finite rise time, $ct_r = H$	22
Fig. 11 -- Comparison of Armour linearized estimate of forces with calculation	24
Fig. 12 -- Comparison of various estimates of the effect of a slow rise, $ct_r = 0.4H$	25
Fig. 13 -- Comparison of various estimates of the effect of a slow rise, $ct_r = H$	26
Fig. 14 -- Comparison of calculation with shock-tube results	28

ON THE EFFECT OF SLOW RISE TIMES ON THE BLAST LOADING OF STRUCTURES

Statement of the Problem

Since the results of Operation BUSTER brought the matter drastically to our attention, it has become more and more evident that shock waves do not always have the ideal behavior described in textbooks (Fig. 1a). A shock wave is usually described as a pressure wave characterized by an almost instantaneous rise in pressure. That such waves do exist there is no doubt; they have been observed repeatedly and used both in experiments with shock tubes and with high explosives. On the other hand, while such waves may result from a nuclear explosion they do not always. In retrospect, nonideal shock fronts can be read into some pressure records from nearly every full-scale operation from SANDSTONE on.

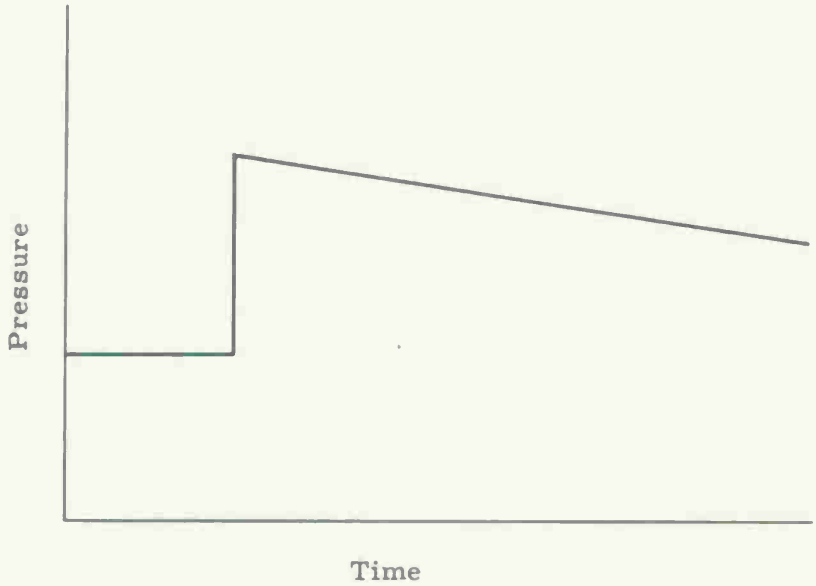

Fig. 1a -- Ideal shock wave

Several possible explanations of nonideal shock waves have been proffered, of which the hot-layer theory developed simultaneously at NOL[1] and elsewhere[2, 3] seems most satisfactorily to describe observed phenomena. This theory postulates an interaction between the ground and thermal radiation from the bomb which results in a layer of hot air along the ground in front of the advancing shock wave. Through this high velocity channel energy leaks out and forms a precursor, which, as its name implies, is a wave running before the

principal shock. In the earlier stages of development the precursor and principal shocks are separate, and a gauge in this region will respond first to one and then to the other, yielding a pressure time wave as in Fig. 1b. As the shock travels further from the explosion, together with a decrease in pressure goes a difference in the character of the precursor phenomenon. The precursor merges with the principal shock, yielding a single-pressure wave, not an ideal shock with a sharp front but one with a slow rise time and rounded peak (as in Fig. 1c) whose properties vary with the height from the ground.

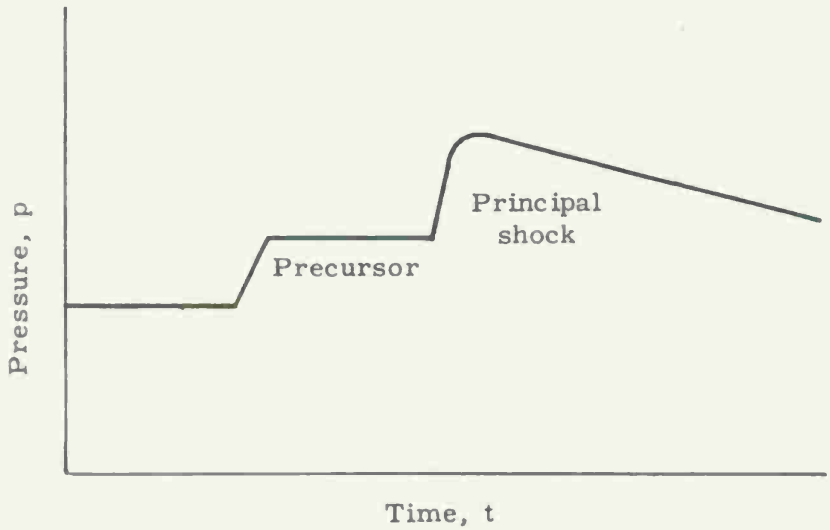

Fig. 1b -- Typical gauge record in the early precursor region

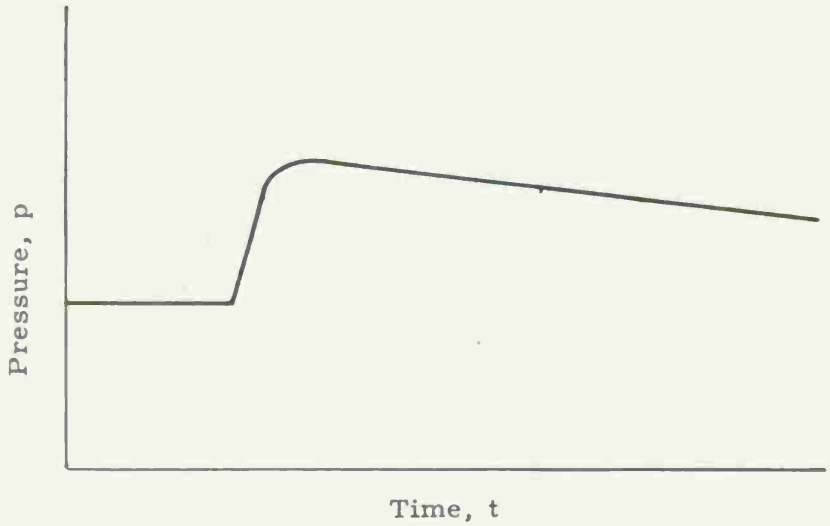

Fig. 1c -- Typical gauge record in the late precursor region

The state of knowledge of the precursor is at present in the yes-or-no stage; one can predict whether or not a precursor will arise under a particular set of burst conditions, but cannot predict with confidence the degree to which it will affect pressure waves. Indications are that the stage represented in Fig. 1b will be present in the 60 to 20 psi overpressure range, while that in Fig. 1c will obtain in the 12 to 8 psi overpressure range. The intermediate 20 to 12 psi range will divide itself between the two ranges in a manner depending on the burst height and yield of the weapon.

A question of considerable importance in the projected use of nuclear weapons is how the degradation of blast waves by precursors will affect the loading and hence the response of structures exposed to them. It is a very difficult question, one to which this report does not propose to give a complete answer: the intention is to attack a part of the problem that can be treated in the hope that a partial answer will help the complete answer to come sooner.

In the present report only the lower range of pressures is considered, principally because it is easier conceptually, although fortunately it includes a large fraction of the number of structures of military interest. (The only kind of above-ground structure whose index of vulnerability[12] exceeds 14 psi is reinforced concrete structures of earthquake-resistant design.) The incident wave is treated as if it were a plane wave perpendicular to the ground, at least in the neighborhood of the structure in whose loadings one might be interested. For the sake of the present argument let it be assumed that it is possible to estimate reasonably well the loads resulting from pressure waves with zero rise time, so that the only remaining difference between the nonideal and the ideal shock wave is in the front itself. Therefore, the phenomenon in Fig. 1c has been idealized to that in Fig. 2, to wit, a flat-topped wave with a linear rise in pressure to its maximum. This pressure wave is fully described by the rise time and by the ratio of the overpressure of the wave, p, to the ambient air pressure, P_o.

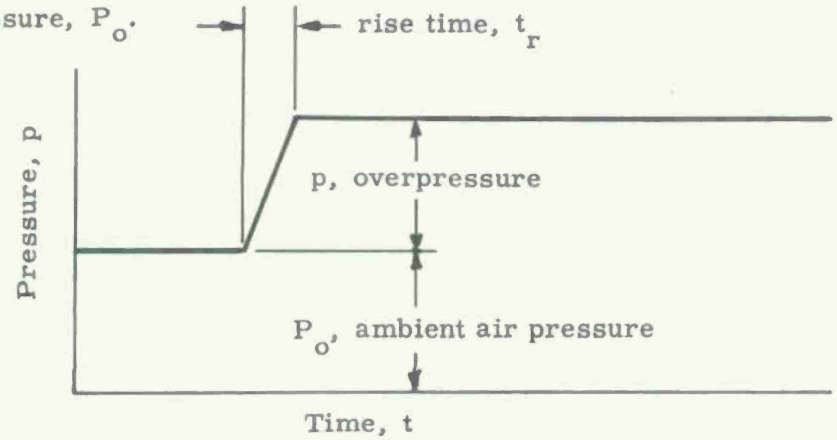

Fig. 2 -- Idealization of nonideal shock wave

For one particular instance one can calculate the loads such a wave would produce on a structure, using the sound-pulse theories developed by Friedlander[4] and by Keller and Blank.[5] This is the case in which the overpressure, p, is much smaller than the ambient pressure, P_o, and the loads are measured about the central portion of a long (or two-dimensional) building struck normally by the blast wave. The loads in these cases can be determined exactly for early times and approximately for a short while thereafter. The purpose of this report is to consider how such wave fronts will influence the loads on structures subject to them. We shall present and discuss the results of calculations in the acoustic case and shall estimate their applicability to finite shocks under actual conditions.

The Sound-Pulse Theories

Independent theories have been developed by Friedlander[4] and by Keller and Blank,[5] each of which describes the diffraction and reflection of sound pulses by wedges. In each it is necessary to find a solution of the wave equation subject to appropriate conditions at the surfaces of the wedge and to the presence of incident and reflected waves. The nature of such an interaction of a sound pulse with a wedge is indicated in Fig. 3: in region I only the incident wave is present, in region II there is also a reflected wave, and in region III a centered rarefaction and compression describes the effect of the corner.

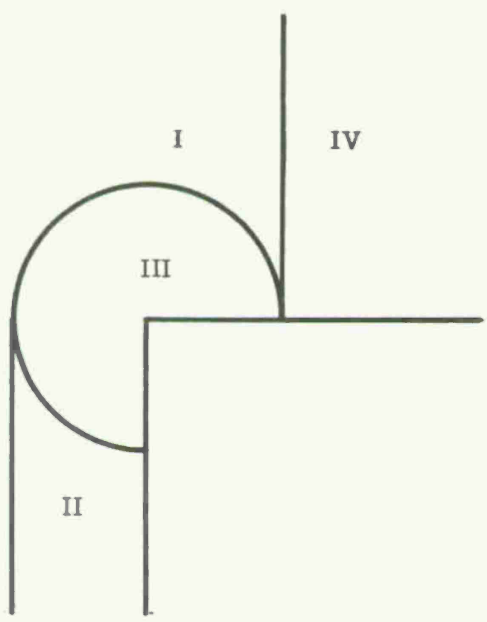

Fig. 3 -- Interaction of a shock wave with a wedge

Keller[5] solves the problem of distribution of pressures in region III by performing a conical transformation on the wave equation, resulting in a problem which can, in principle, be solved by the usual methods of potential theory. To extend the results to other than flat-topped pressure waves, Keller employs Duhamel's Theorem. Friedlander's solution[4] is based on a much earlier paper by Sommerfeld on X-ray diffraction.[6] Although the concepts expressed are not as clearly evident as in Keller's paper, the results are expressed as a definite integral involving the shape of the incident pulse; and for this reason, Friedlander's formulation is used as the basis of this report. That Friedlander's and Keller's methods give the same answers we have assumed from the Uniqueness Theorem and the identity of boundary conditions, but have not succeeded in showing the results to be mathematically identical.

For a right-angled wedge, Friedlander's expressions can be manipulated to describe the compression-rarefaction wave in region III in the form:

$$p = \int_0^\infty P(ct - r \cosh b)\, q'(b)\, db, \tag{1}$$

where

$$q(b) = -\frac{1}{\pi}\tan^{-1}\left\{\frac{\sin 2\pi/3 \sinh 2b/3}{\cos 2(\phi - \phi')/3 - \cos 2\pi/3 \cosh 2b/3}\right\}$$

$$-\frac{1}{\pi}\tan^{-1}\left\{\frac{\sin 2\pi/3 \sinh 2b/3}{\cos 2(\phi + \phi')/3 - \cos 2\pi/3 \cosh 2b/3}\right\},$$

and

$$q(0) = 0.$$

In this formula ϕ is the angle of measurement (0° and 270° on the surfaces of the wedge in Fig. 3) and ϕ' is the direction of travel of the incident wave (180° in Fig. 3). The expression, $P(ct - r \cos(\phi - \phi'))$, describes the incident wave in regions I and IV. When $\phi' = 0$ the two terms in $q(b)$ are alike and only one is used.

For a simple step-function wave ($t_r = 0$ in Fig. 2) equation 1 becomes

$$p = \int_0^{b_2} q'(b)\, db = q(b_2),$$

where

$$b_2 = \cosh^{-1} ct/r.$$

The interesting and useful aspect of this solution is that the time and space variables always occur in the combination ct/r:

(2) $$p = p\,(ct/r,\ \phi,\ \phi').$$

These functions have been calculated for the conditions,

$$\phi = 0,\ 270^{\circ};$$

$$\phi' = 0,\ 180^{\circ};$$

and are plotted in Figs. 4a and 4b.*

If, instead of being a simple step function, the incident wave takes a time $ct_r = a$ to rise to the flat top, we have

(3) $$\begin{aligned} P(z) &= 0 & z &\leq 0 \\ P(z) \text{ not specified} & & 0 < z &< a \\ P(z) &= 1 & z &\geq a \quad . \end{aligned}$$

Thus for $ct - r \leq a$, equation 1 becomes

$$\tilde{p} = \int_0^{b_2} P(ct - r\cosh b)\, q'(b)\, db\ .$$

Integrating by parts we get

$$\tilde{p} = P(ct - r\cosh b)\, q(b) \Big|_0^{b_2} + \int_0^{b_2} P'(ct - r\cosh b)\, q(b)\, d(r\cosh b)\ .$$

The first term vanishes at both limits. In the second term, substituting $\xi = r\cosh b$ we get

(4a) $$\tilde{p} = \int_r^{ct} P'(ct - \xi)\, p\,(\xi/r)\, d\xi\ .$$

If, on the other hand, $ct - r \geq a$ we would have arrived at the expression,

(4) $$\tilde{p} = \int_{ct-a}^{ct} P'(ct - \xi)\, p(\xi/r)\, d\xi\ .$$

---

*In these figures, and hereafter, all overpressures are expressed as normalized pressures, p/p_m, ie, divided by the strength of the incident wave.

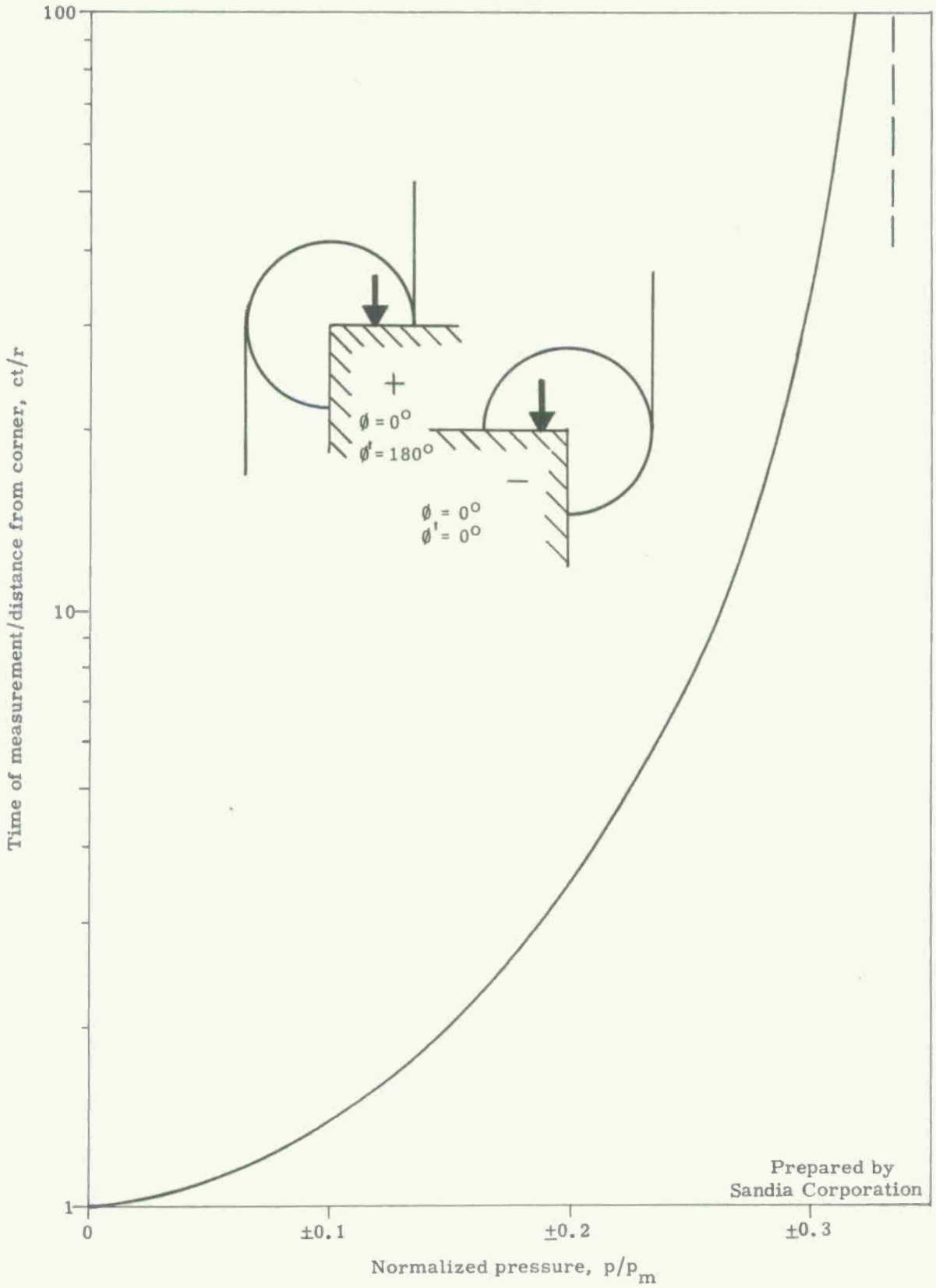

Fig. 4a -- Diffraction pressure corrections for top of wedge

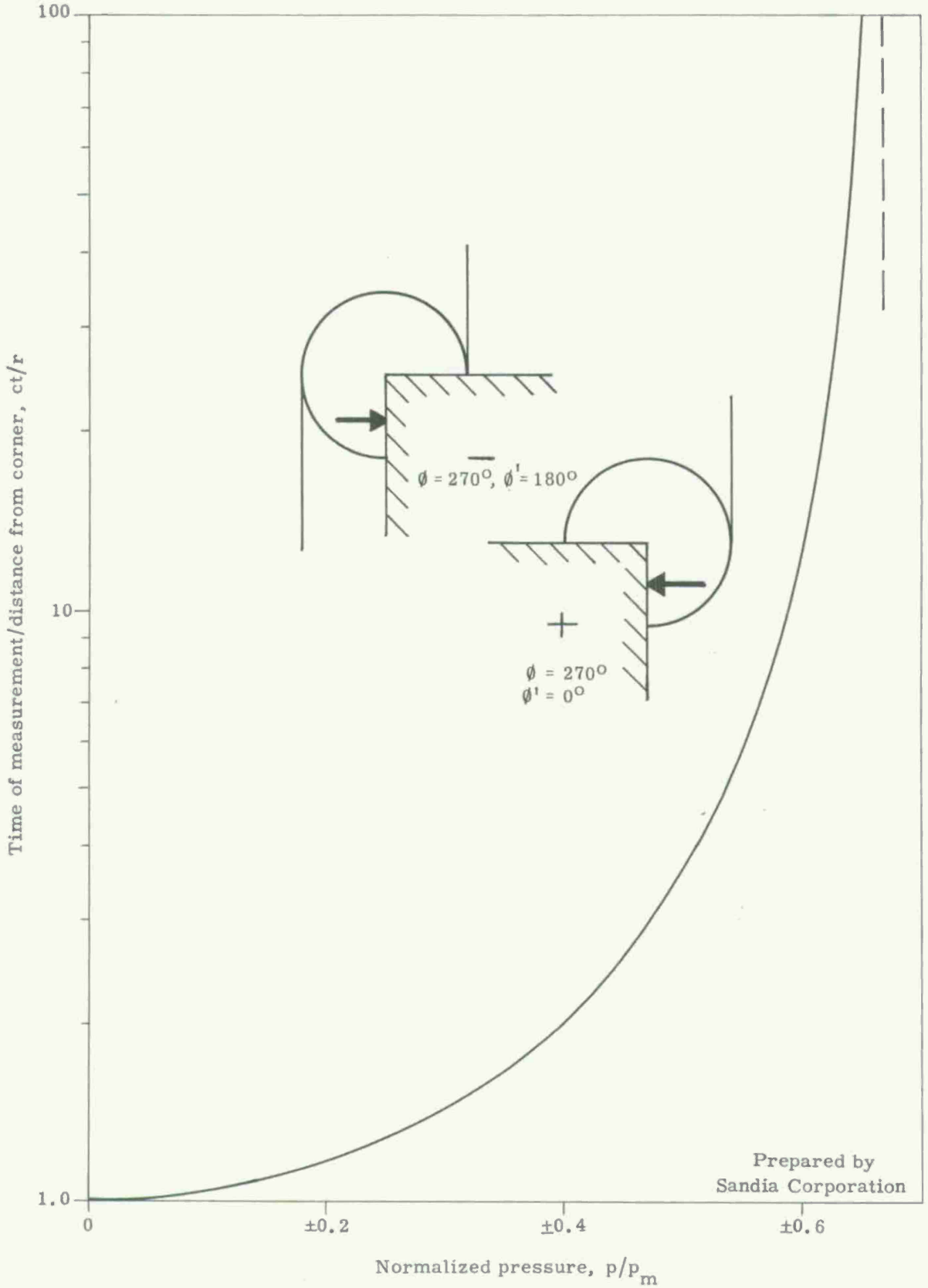

Fig. 4b -- Diffraction pressure corrections for front and back of wedge

This expression is actually equivalent to equation 4a because of the condition that

$$P(z) = 0 \qquad z \leq 0 ,$$

so it will be used henceforth.

The physical meaning of equation 4 is that if the rise is not instantaneous then the resultant pressure at a point is an average of $p(ct/r)$ over the range from $ct - a$ to ct, weighted according to the factor $P'(ct - \xi)$.

Thus, if the rise is a double jump $P'(z)$ becomes the sum of two Dirac delta functions, and the resulting strength of the diffracted wave at any point is the arithmetic average of the values $p(ct/r)$ and $p(ct-a/r)$. Again, if the rise is a linear rise,

$$\begin{aligned} P(z) &= 0 & z &\leq 0 \\ P(z) &= z/a & 0 < z &< a \\ P(z) &= 1 & z &\geq a \quad , \end{aligned} \tag{5}$$

then $P'(z) = 1/a$, and the resultant pressure becomes the average value of all values of $p(ct/r)$ between $ct-a$ and ct.

The conclusion expressed in equation 4 is a very important one, essential to the whole of the following argument.

Application of the Theory

As it stands the sound-pulse theory is applicable only to infinite wedges. Fortunately, however, acoustic theory is a linear theory: it admits direct superposition of solutions. This fact will be used to make the results indicated above apply to a two-dimensional building. To illustrate its use let us consider a building whose length in the radial direction is twice its height.

A space-time plot for such a building is outlined in Fig. 5. The vertical scale represents position and the horizontal scale, time. No pressure contours are shown, but the lines A to C represent waves traveling over various portions of the structure.

When an acoustic shock strikes and reflects from such a structure the pressure on the front doubles (area I, Fig. 5). The wave front of the rarefaction relieving this pressure is seen as line A. Lines B and C represent the shock fronts traveling over the top and back faces of the building. In regions II and III the pressure distribution

AFSWP-460

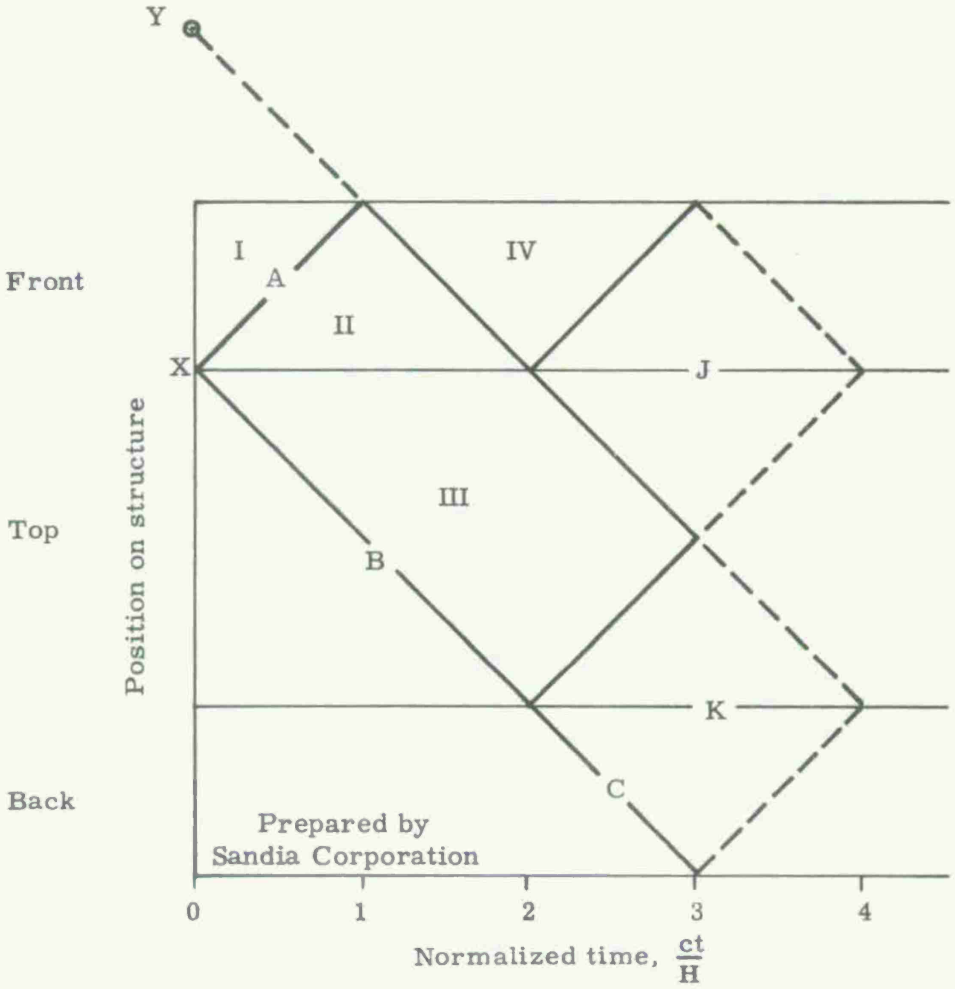

Fig. 5 -- Space-time plot of pressures on a 2:1 building

consists of a superposition of a wave centered at X on a constant pressure of 2 in region II and 1 in region III. In region IV the reflection of the rarefaction must also be considered; it appears as a rarefaction wave centered at Y, which is the point X imaged in the ground.

In regions I to IV the pressure is known exactly, but not in any other region. Sound-pulse theory at present permits the calculation only of the diffraction of a plane wave, and regions like that to the right of C have the contribution of the diffraction of nonplane waves. Nevertheless, the values of pressures along the lines J and K are known up to time ct = 3H* because of the interesting and useful fact (Fig. 4) that a centered diffraction wave approaches the value 2/3 of the incident pressure at the apex of a right-angle wedge on which it is impinging. Thus, the value of pressure along the line J is

2 for the reflection on the front face,
less 2/3 for the wave centered at X,
less 2/3 of the wave centered at Y.

The force or average pressure on any surface of the structure can be obtained from Fig. 5 by averaging over a vertical line. It can be calculated exactly for all times, $ct \leq 2H$, and can be estimated for $ct \leq 3H$.

A detailed space-time plot for a step-function acoustic shock (equation 6) is shown in Fig. 6. Pressure profiles derivative from it are shown in Fig. 7, and are integrated to get the force-time curves shown in Fig. 8.

Figure 8 shows that the initial portions of the force-time curve are linear. That such a thing is reasonable can be seen as follows.

From Fig. 6 it is evident that, $p(ct/r,\ 270^\circ,\ 180^\circ)$ being a wave centered at X, the force on the front is

$$F_F(t) = 2 - \frac{1}{H}\int_0^{ct} p(ct/r,\ 270^\circ,\ 180^\circ)\,dr \tag{6}$$

$$= 2 - \frac{ct}{H}\int_0^{1} p(1/\xi,\ 270^\circ,\ 180^\circ)\,d\xi\ .$$

Thus, initially the force on the front face decreases linearly with time as shown in Fig. 8.

---

*It is convenient to express times as normalized times, ct/H, ie, divided by the time necessary for the shock to travel a distance equivalent to the height of the structure.

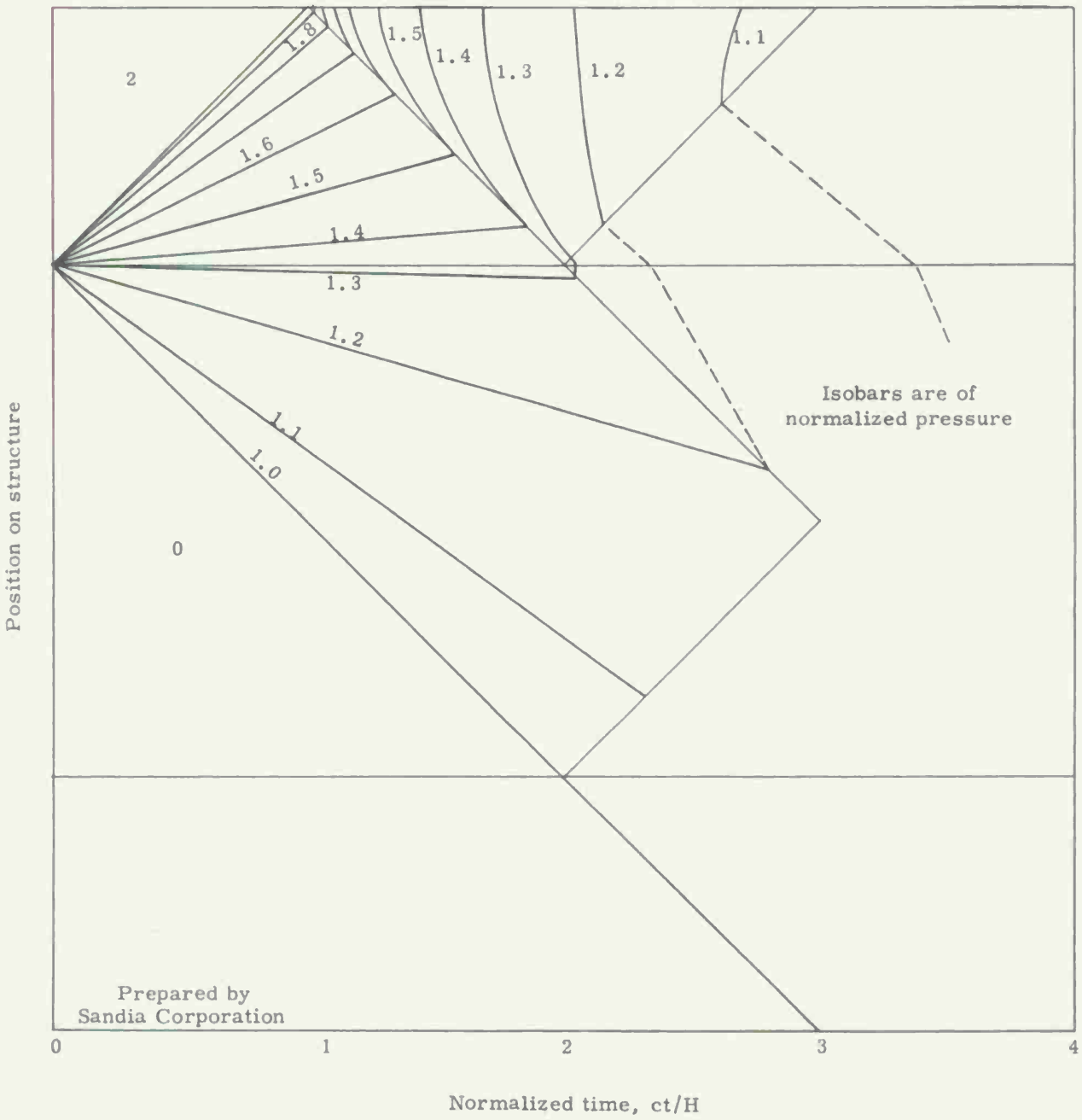

Fig. 6 -- Space-time plot of loading on a 2:1 building

Fig. 7 -- Pressure profiles of loading on a 2:1 building

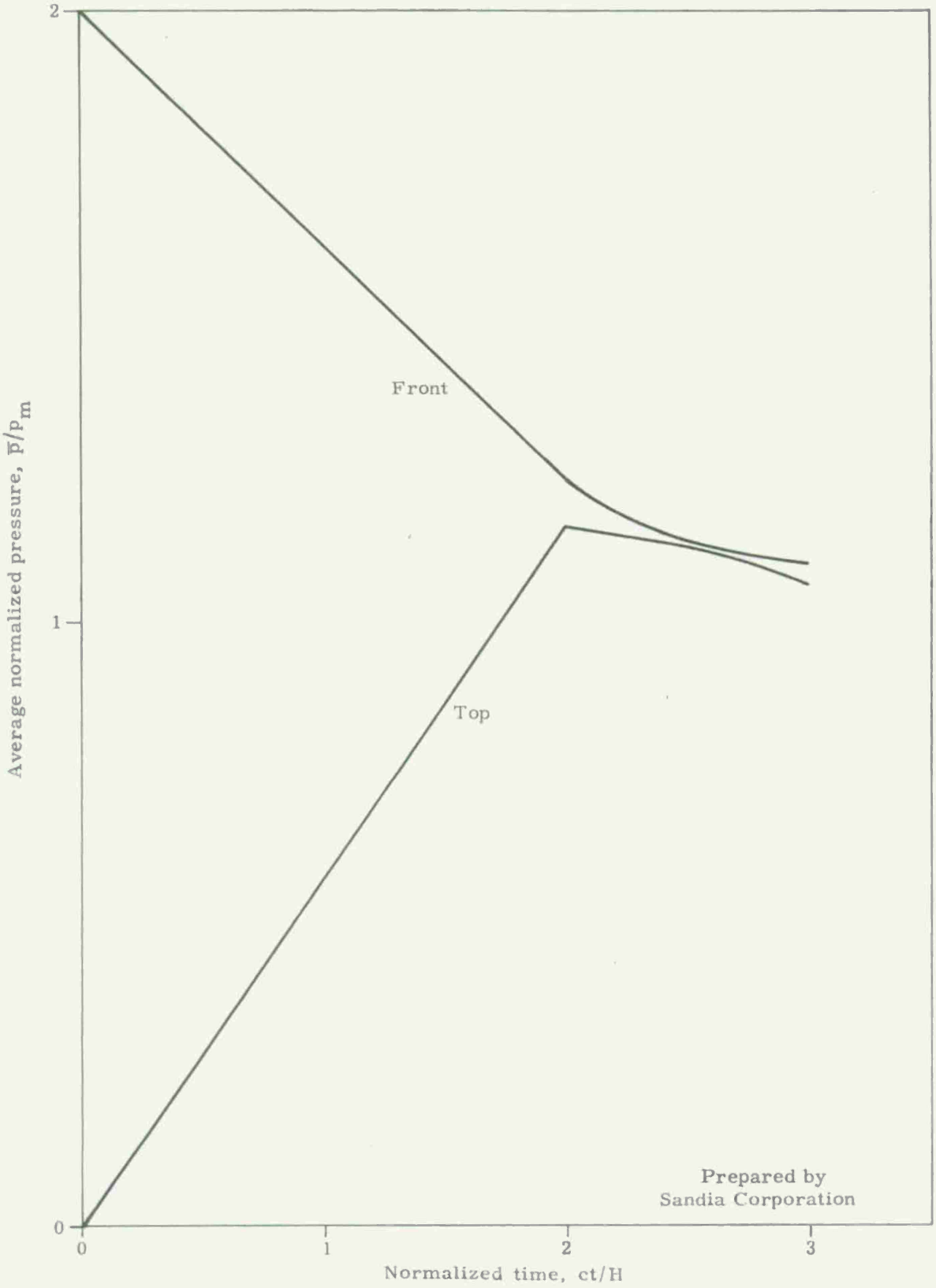

Fig. 8 -- Forces on the front and top of a 2:1 building

Similarly, on the top:

$$F_T(t) = \frac{ct}{L}\left\{1 + \int_0^1 p(1/\xi,\ 0^\circ,\ 180^\circ)\, d\xi\right\}, \tag{7}$$

and the force on the top face increases linearly with time.

This whole process could be repeated for other types of waves, especially that of Fig. 2. However, an analysis based on equation 4 shows that this process is not necessary. If the forces on the various faces of a structure are known for an incident wave with an abrupt rise, a step-function incident wave, the forces for incident waves with other rises can be derived from the first in a simple manner analogous to that of equation 4. We shall demonstrate that this result applies exactly for early times and infer that it also applies for later times.

Using equation 4 in an equation of the form of equation 6, we find that the total force on the front face becomes

$$\begin{aligned}
\tilde{F}_F(t) &= 2\,P(t) - \frac{1}{H}\int_0^{ct} \tilde{p}\, ds \\
&= 2\int_{ct-a}^{ct} P'(ct-\xi)\, d\xi - \frac{1}{H}\int_0^{ct}\int_{ct-a}^{ct} P'(ct-\xi)\, p(\xi/s)\, d\xi\, ds \\
&= \int_{ct-a}^{ct} P'(ct-\xi)\left\{2 - \frac{1}{H}\int_0^{ct} p(\xi/s)\, ds\right\} d\xi\ ;
\end{aligned}$$

and thus,

$$\tilde{F}_F(t) = \int_{ct-a}^{ct} P'(ct-\xi)\, F_F(\xi)\, d\xi\ . \tag{8}$$

The same result can be shown for the top face.

We have therefore come to the conclusion, expressed analytically in equation 8, that total forces on the various faces of a structure are related to the same forces resulting from a step-function wave by a simple weighted average, whose weights depend on the method of rise of the incident-pressure pulse. This conclusion has been verified for early times, $ct \leq 2H$, and it is a logical induction to expect that it should be true for later times, it only being necessary to assume that all later pressures can be expressed as the sum or integral of a finite number of centered waves.

The Effects of a Slow Rise

In Fig. 8 we have seen what the loads will be on a 2:1 structure if struck by a step-function wave. Let us apply the methods of equation 8 to those results and find out what these loads will be like if the structure is struck by a slow rise wave.

At this point we must assume a rise time and relate it to the time scale already being used, one based on the structural dimensions. For the sake of example let us assume two values: $a = ct_r = .4H$ and $a = H$. (The first might, for instance, represent a a wave with a rise time of 10 msec impinging on a structure 30 ft high.) The results are shown in Figs. 9 and 10. It is evident that the maximum pressures on all faces are lowered and delayed, the longer the rise time the greater the effect. Actually, the reduction of pressure is not unexpected, and the assertion that it must be so has been used as an argument that slow rise waves may not be as damaging as step-function waves of the same amplitude.

Comparison with Previous Estimates

In the course of the development of the art various empirical means have been devised for estimating blast loads on structures and for correcting these estimates for the effects of finite rise times. We wish here to compare these estimates with the results expressed in Fig. 8 and equation 8.

A linearized estimate has been developed by Armour Research Foundation,[7] which is based on shock-tube data and information on the Air Force structures in GREENHOUSE. In this estimate the front face load is approximated by two lines, one representing the pseudo-steady state pressure (average pressure due to wind alone) and one a straight line connecting the reflected overpressure at zero point to the first at a time related to the height of the structure and called the clearing time:

$$t_c = 3H/c_r .$$

Top face pressures are approximated by two lines, one again being the pseudo-steady state pressure and the other a straight line joining the zero zero point with the first line at a time related to the length of the structure:

$$t = L/U .$$

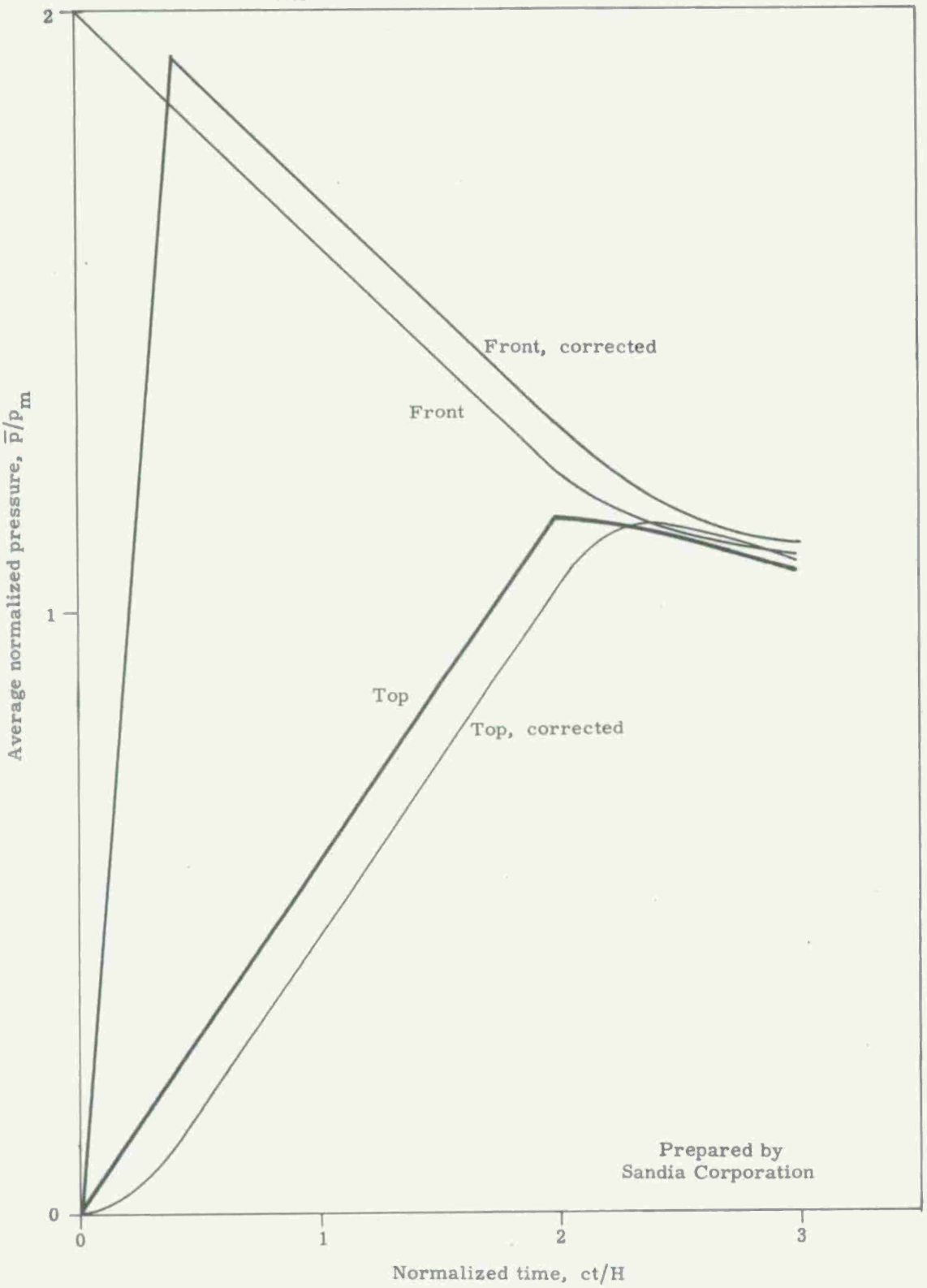

Fig. 9 -- Correction of forces for a finite rise time, $ct_r = 0.4H$

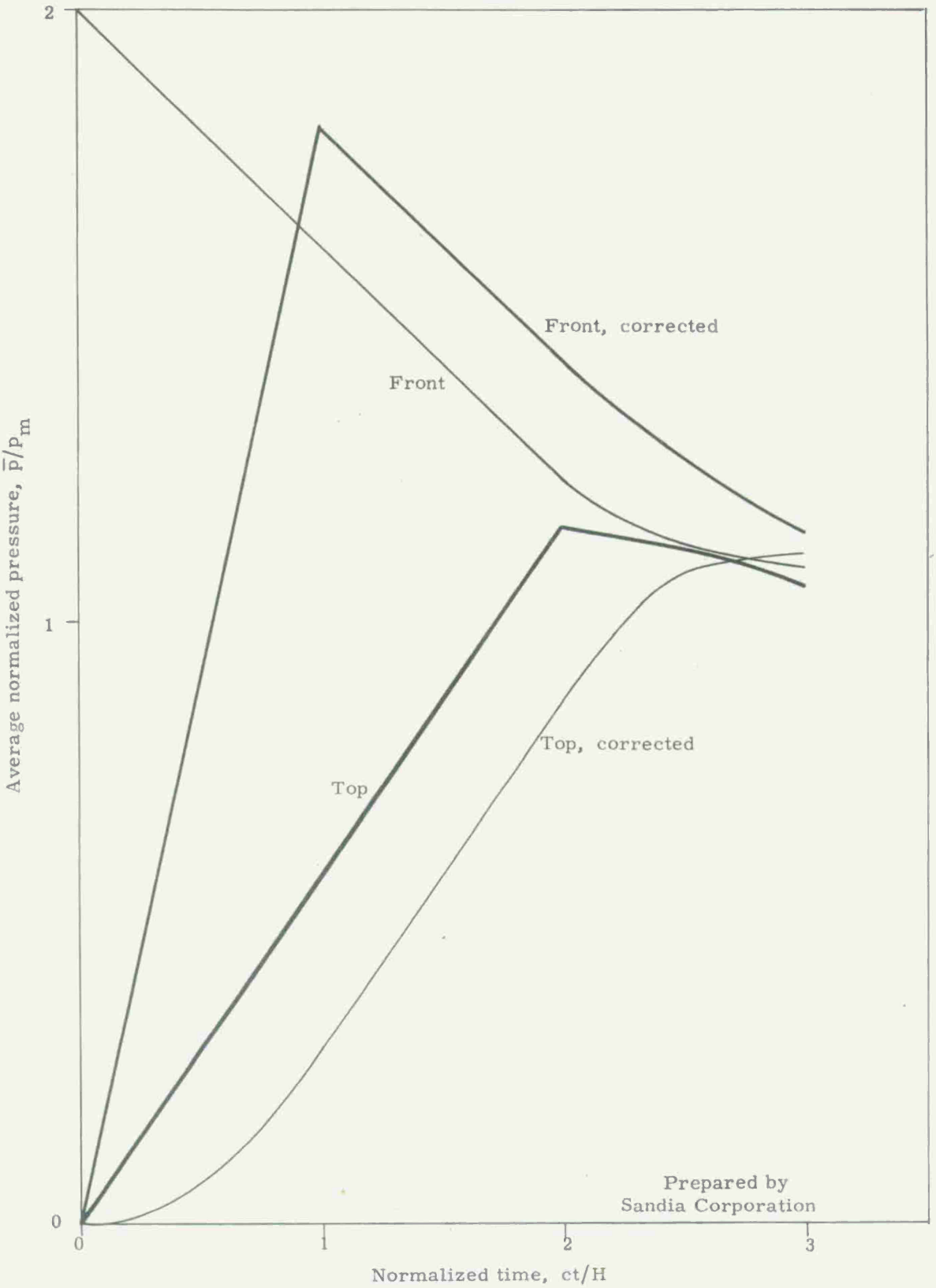

Fig. 10 -- Correction of forces for a finite rise time, $ct_r = H$

In Fig. 11 this estimate is compared with the calculation. The extent of disagreement is not large and would probably seem less if the time scale were compressed. This same estimate has been adopted by M. I. T. for use in a forthcoming manual on protective construction.[8] We in the Sandia Corporation have suggested a somewhat different estimate[9] also based on shock-tube data. The differences between it and the Armour estimate are principally a matter of method and detail. The Sandia estimate will agree with the calculation from sound-pulse theory because it was in part based on that calculation.

To correct for the effect of a slow rise time on front-face loads, Armour suggests drawing a third line from zero zero to a point representing a pressure equal to the reflected pressure at a time equal to the rise time. The area remaining under the several curves is taken as the estimate of loading. No correction is made on the top face.

A somewhat related method, which is implied in AFSWP-226, even if not explicitly stated, is to correct for slow rise by drawing a straight line from zero zero to intersect the otherwise predicted loading curve at a time equal to the rise time.

Both of these possible estimates will underestimate the resultant maximum force on the building; or, expressed otherwise, both will overestimate the effect of the slow rise. This can be seen in Figs. 12 and 13, where the calculated load is compared to the other two proposed estimates. The Armour proposal does not make as great an error in maximum pressure level, but it does make an error in the time at which the maximum occurs. The Sandia estimate makes a greater pressure error but no time error (Table I). Neither estimate makes any allowance for the changes in top-face loading implied in Figs. 9 and 10.

TABLE I

Effects of Slow Rise as Predicted and Calculated

	$t_r = .4\ H/C$	$t_r = H/C$
ΔP (calc)	.08	.20
ΔP (ARF)	.12	.29
ΔP (SC)	.15	.38
T_{max}(Calc)	.40	1.00
T_{max}(ARF)	.38	.86
T_{max}(SC)	.40	1.00

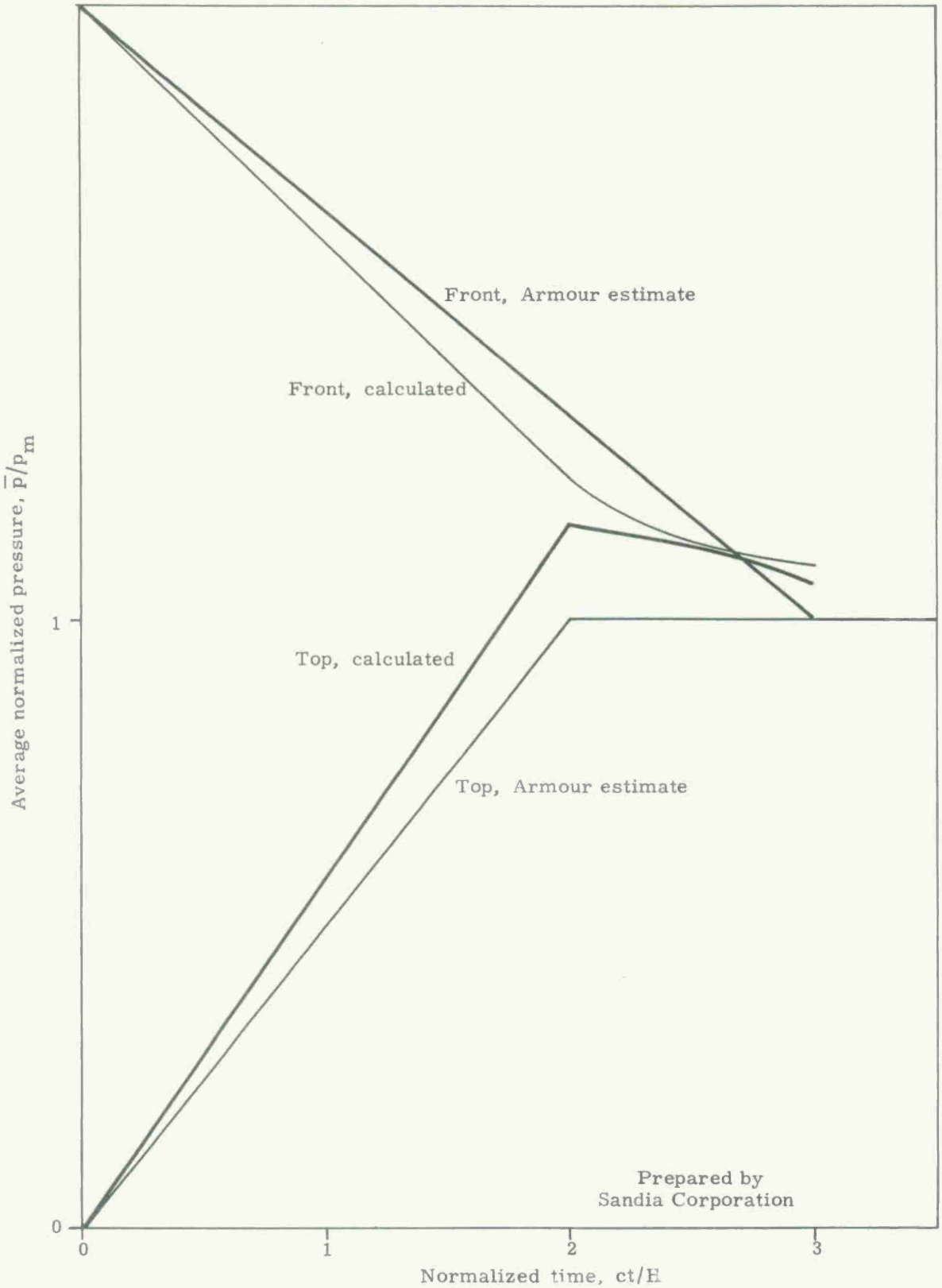

Fig. 11 -- Comparison of Armour linearized estimate of forces with calculation

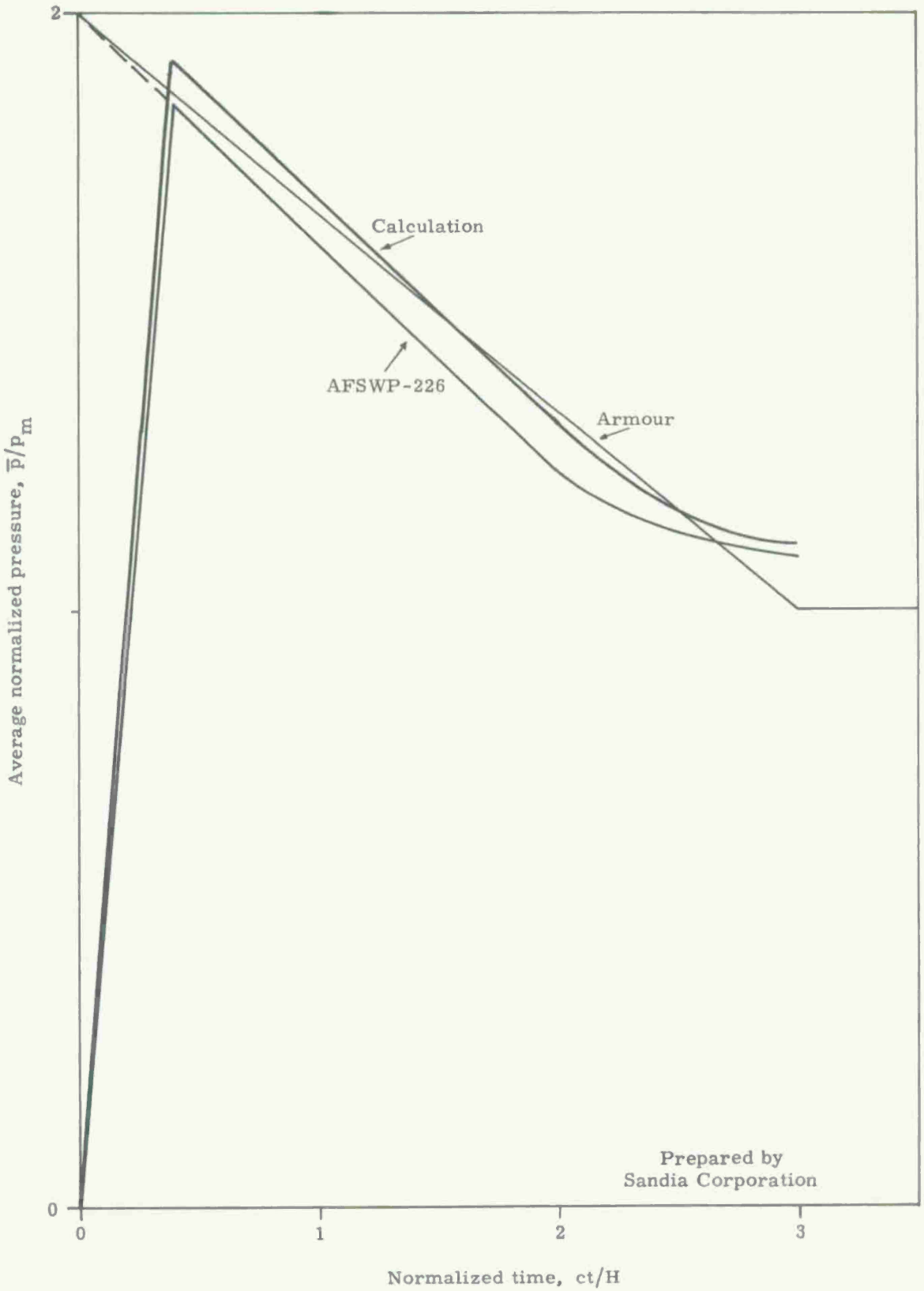

Fig. 12 -- Comparison of various estimates of the effect of a slow rise, $ct_r = 0.4H$

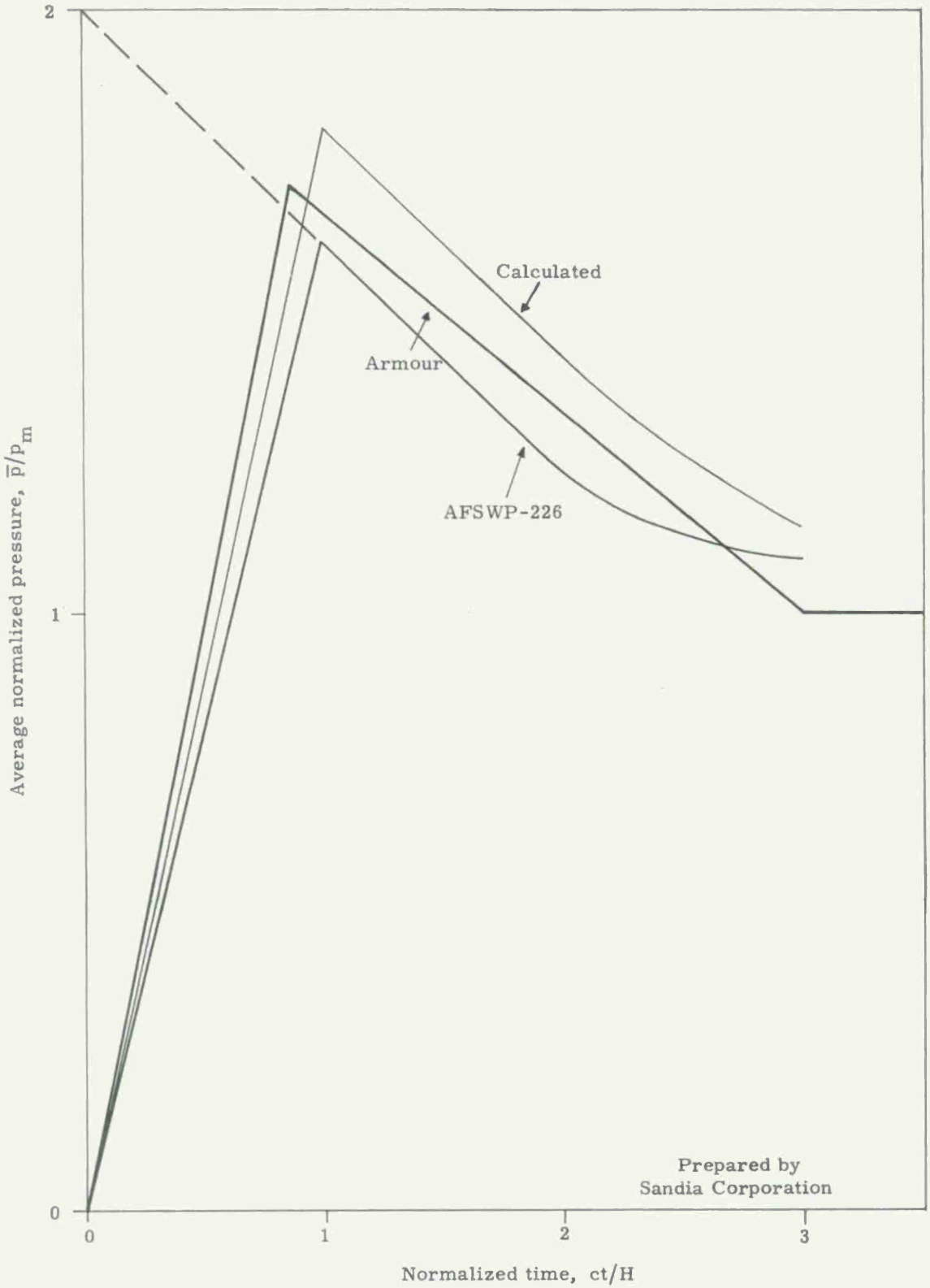

Fig. 13 -- Comparison of various estimates of the effect of a slow rise, $ct_r = H$

Applicability to Finite Shocks under Actual Conditions

A heading such as this implies not only that the effects of slow rise times might be somewhat different for finite shocks than for acoustic shocks, but also that actual conditions might be out of the ordinary in some other respects.

The loading of structures with finite step-function shocks is just the problem to which shock-tube data give an answer.[10] The calculated results for a front surface are compared to some of these data in Fig. 14. The most obvious departure of finite shocks from the calculated result of an acoustic shock is in the initial reflected pressure on the front face. This correction is easily made by using the reflection factor for finite shocks:

$$\text{R.F.} = 2\left\{\frac{7P_o + 4\,p}{7P_o + p}\right\} .$$

Thereafter the forces from finite shocks decrease in an approximately linear manner, although possibly with a slightly different slope than in the acoustic case.

That the simple result of equation 8 is true depended upon the various diffraction waves being centered waves (ie, describable in the form $p(ct/r)$) and that the acoustic theory results in a linear integral equation. There is every reason to expect that finite shocks, being in other respects nonlinear, will not yield diffraction loadings in such simple linear forms as equation 1. On the other hand, it is certainly probable that for finite but weak shocks, such a form will serve as an approximation, the undetermined exact form differing from it by terms of the order of p/P_o or smaller. We are therefore inclined to use equation 8, as it stands, for weak but finite shocks, say for

$$p/P_o \leq 0.7 .$$

Another respect in which blast waves in general differ from those hitherto assumed is that the pressure in such waves decreases after reaching its maximum instead of staying constant. An argument similar to that already given shows that if two shock waves differ only in their rise times, results analogous to equation 4 and 8 apply. Thus, if $P_1(z)$ is a pressure wave with a zero time of rise, and $P_2(z)$ is identical except for a finite rise time, t_r, then their ratio, $g(z)$, has the properties listed in equation 3, so that the result of equation 4 is valid, providing the expression P' is replaced by g':

$$\tilde{p} = \int_{ct-a}^{ct} g'(ct - \xi)\, p(\xi/r)\, d\xi$$

(4b) $$g(z) = P_2(z)/P_1(z) .$$

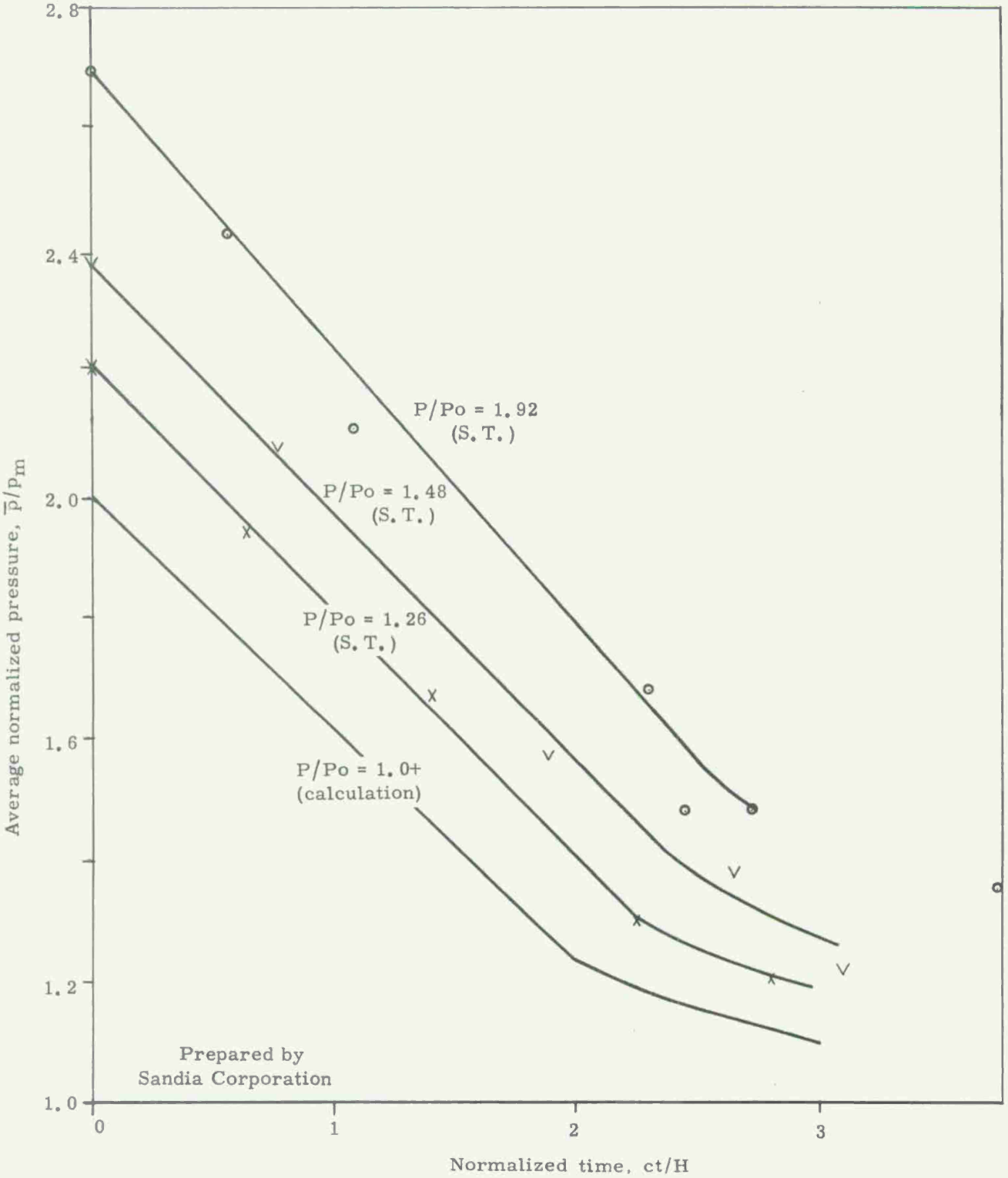

Fig. 14 -- Comparison of calculation with shock-tube results
(shock-tube data from Princeton, Ref 10)

Similarly, equation 8 can be rephrased as

$$\tilde{F}(t) = \int_{ct-a}^{ct} g'(ct - \xi)\, F(\xi)\, d\xi, \tag{8a}$$

where $p(ct/r)$ and $F(t)$ are now the point pressures and total forces resulting from an incident wave, $P_1(z)$.

As derived, these expressions apply only to long buildings of rectangular cross-section and without windows. However, they may be safely used for buildings that are not long, for the effect of the added dimension is only to contribute additional centered diffraction waves. They may also be used for buildings not rectangular in section since relations similar in form to equation 1 can be set up for angles other than right angles. On the other hand, if the structure has any considerable number of openings in it the above expressions probably are no longer valid.

Even more than these things, it is important to remember the practical fact that slow rise times are but one of several effects associated with the formation of a precursor. This one effect has been seized upon because it can be handled; but if only it is taken into account, other equally important effects will be neglected.

When the precursor region is investigated, not by one gauge but by several gauges at various heights above the ground or by photography, the other effects become apparent. The layer of hot air along the ground merges gradually into unheated air above so that the velocity of sound in front of the advancing shock wave varies continuously from normal velocities at considerable heights above the ground to very large values near the ground. The advancing shock is not perpendicular to the surface of the ground but travels toe first. The angle the shock makes with the ground can be very different from a right angle; at early times this angle might be as little as 30°, but by the time the precursor has merged with the main shock, this angle has probably increased to approximately 60°. Together with variable velocities and nonperpendicular wave fronts goes a variation with height of wave shapes and probably of rise times.

We are not prepared to do more than guess what effects these factors have on the loading of a structure. If the sound velocity were the same at all heights above the ground, its effect could easily be accounted for; but under these conditions one is probably forced to use an average velocity, albeit an elevated one. Because of the high-sound velocity the time scale in Figs. 8 through 14 corresponds to a much smaller absolute time scale than

would ordinarily be expected; but on the other hand, a given rise time is relatively much longer and more important than at Standard Temperature Pressure. Similarly, an average wave shape and an average rise time will have to be used.

Neither are we prepared at present to say what would be the effect of the front not being perpendicular to the ground. Fortunately, in the same region where pressures such as we have been discussing occur, the deviation from perpendicularity is rapidly becoming small.

Simultaneously, things are happening behind the front which perhaps ought to be considered in any complete description of the loading of a structure. All the evidence points to great quantities of dust. Obviously, some of this dust will hit any building in its path, perhaps in quantities great enough to affect its motion. Also, preliminary data from Operation UPSHOT-KNOTHOLE indicate that in the precursor region the dynamic pressure, $q = 1/2\ \rho u^2$, does not bear the same simple relation to the overpressure which it does for clean ideal shocks but runs high. This will have an effect principally in the later stages of loading because in the earlier stages other factors, in particular the reflection factor, are more important.

All of this discussion is intended to point out that the problem of the loading of structures by precursor-type waves is a very complicated problem indeed. Possibly its solution will never be entirely satisfactory. Nevertheless, it can be approached by the time-tried method of considering each factor separately to see what will be its effects.

Conclusions

The effects of precursor-type wave forms on the loading and hence the response of structures is a matter of considerable interest in any projected use of nuclear weapons. In this report we have concentrated on one part of the larger problem, on the effects of the slow rises to their maxima of the pressure in blast waves. A rule has been developed for their effects which is exact in the acoustic case and approximate for finite shocks.) is embodied in the integral:

$$\widetilde{F}(t) = \int_{ct-a}^{ct} g'(ct - \xi)\, F(\xi)\, d\xi \ ,$$

where

$F(t)$ = load on a portion of a structure resulting from the incidence of an ideal shock, one with zero rise time;

$g(z)$ = the ratio of the nonideal shock actually incident on the structure to the ideal, where the nonideal differs from the ideal only by having a finite time of rise, t_r;

$\tilde{F}(t)$ = load on a portion of a structure resulting from the incidence of the nonideal shock.

For a linear rise this rule amounts to averaging an ideal force between times $t - t_r$ and t. In general, the effect of a slow rise is to decrease and delay the maximum force applied to a structure.

The application of this rule is limited to shocks of overpressure less than 10 psi and rise times less than twice the time necessary for the shock to travel a distance equal to the height of the structure, $ct_r < 2H$. The rule may be applied as it stands to any structure having few windows which is struck normally by a blast. The rule may not safely be used for structures of the so-called drag-sensitive type.

It must be emphasized that slow rise times appear together with other extraordinary phenomena. These other effects include a variation of sound velocity and wave form with height above the ground, an inclination of the wave front to the ground, and considerable quantities of dust behind the shock front. Indeed, the proposal of the rule itself is somewhat academic since as yet there is no good way to foresee what will be any of the properties of a precursor in a given situation.

During the course of the argument it was shown possible to derive the loading of structures by acoustic shocks without reference to experiment. This matter is of interest in that such a result forms the limiting case of the loading of structures by successively weaker shocks. (That it does indeed provide such a limit has been shown for one case by Keller.[11]) This exact calculation was compared with Armour's linearized approximation and the disagreements were found to be minor.

LIST OF REFERENCES

1. Aronson, C. J., et al., Free-Air and Ground-Level Pressure Measurements, November 6, 1952, WT-513.

2. Shelton, F. H., The Precursor, Its Formation, Prediction and Effects, Sandia Corporation, July 27, 1953, SC-2850.

3. Porzel, F. B., Height of Burst for Atomic Bombs, to be pub., LA-1406.

4. Friedlander, F. G., "The Diffraction of Sound Pulses", Proc. Roy. Soc., A 186, 322 (1946).

5. Keller, J. B. and Blank, A., "Diffraction and Reflection of Pulses by Wedges and Corners", Comm. Pure and Appl. Math., 4, No. 1, 75-94 (June 1951).

6. Sommerfeld, A. "Theoretische Beugung der Roentgenstrahlen", Z. f. Math. Ph., 11 (1901).

7. Armour Research Foundation, "General Blast Loading and Response", Air Force Structures Project 3.3., OPERATION GREENHOUSE, March 1951, Appendix E, I.

   Armour Research Foundation, "Blast Loading and Response of Structures", Air Force Structures Program, Project 3.3, OPERATION GREENHOUSE, May 1952, Appendix I, I.

8. M.I.T., Principles of Atomic Weapon Resistant Construction, to be pub., Chapter 3.

9. Vortman, L. J. and Merritt, M. L., Methods for Predicting Blast Loads on Simple Structures, Sandia Corporation, September 1953, AFSWP-226.

10. Bleakney, W., Shock Loading of Rectangular Structures, Princeton U. Tech. Report II-11 (AFSWP-140), January 10, 1952.

11. Keller, J. B., "Diffraction of a Shock or an Electromagnetic Pulse by a Right Angled Wedge", J. Appl. Ph., 23, 1267 (1952).

12. AFSWP, Capabilities of Atomic Weapons, October 1952, TM 23-200.

AFSWP-460

INITIAL DISTRIBUTION

1 R. E. Poole, 1000
2 W. A. MacNair, 5000
3 R. W. Henderson, 1200
4 L. A. Hopkins, 1300
5 L. J. Paddison, 1500
6 A. B. Machen, 1700
7 S. C. Hight, 5100
8 G. A. Fowler, 5200
9 F. J. Given, 5300
10 L. G. Abraham, 5400
11 E. F. Cox, 5110
12 R. W. Shephard, 5120
13 K. W. Erickson, 5130
14 G. E. Hansche, 5140
15 M. L. Merritt, 5111
16 J. D. Shreve, 5112
17 G. T. Pelsor, 5121
18 W. E. Boyes, 5131
19 S. H. Dike, 5133
20 L. J. Vortman, 5112-1
21 J. von Neumann, IAS, Princeton
22 W. Bleakney, Princeton University
23 C. W. Lampson, BRL
24 G. K. Hartmann, NOL
25 H. C. Hottel, MIT
26 F. Reines, LASL
27 F. B. Porzel, LASL
28 W. E. Ogle, LASL
29 R. J. Hansen, MIT
30 R. M. Newmark, U. Ill
31 E. B. Doll, SRI
32 H. W. Bode, BTL
33 M. V. Barton, U. Tex
34 P. Fine, DMA/AEC
35 C. Beck, Construction Div, AEC
36 R. L. Corsbie, DBM/AEC
37 H. L. Bowman, DBM/AEC
38-47 Document Room

(Through Col. J. H. Veyette)

ARMY

48 Asst Chief of Staff, G-2, D/A, Washington 25, DC
49 Asst Chief of Staff, G-3, D/A, Washington 25, DC
ATTN: Dep. Chief of Staff, G-3, (RR&SW)

INITIAL DISTRIBUTION (cont)

50 Asst Chief of Staff, G-4, D/A, Washington 25, DC
51 Chief of Ordnance, D/A, Washington 25, DC
ATTN: ORDTX-AR
52-54 Chief Signal Officer, D/A, P&O Div, Washington 25, DC
ATTN: SIGOP
55 The Surgeon General, D/A, Washington 25, DC
ATTN: Chairman, Med R&D Board
56-57 Chief Chemical Officer, D/A, Washington 25, DC
58 Asst Chief of Engineers for Troop Operations, Office of the Chief of Engineers, Dept of the Army, Washington 25, DC
59 Chief of Engineers, D/A, Military Construction Div, Protective Construction Br, Washington 25, DC
ATTN: ENGEB
60 Chief of Engineers, D/A, Civil Works Div, Washington 25, DC
ATTN: Engineering Div Structural Br
61 The Quartermaster General, CBR, Liaison Officer, R&D Div, Department of the Army, Washington 25, DC
62 Chief of Transportation, Military Planning & Intelligence Div, Washington 25, DC
63-69 Chief, Army Field Forces, Fort Monroe, Va
70 Board #1, OCAFF, Fort Bragg, NC
71 Board #2, OCAFF, Fort Knox, Ky
72 Board #4, OCAFF, Fort Bliss, Tex
73-77 Commanding General, First Army, Governors Island, NY 4, NY
ATTN: G-1 (1 copy)
G-2 (1 copy)
G-3 (1 copy)
G-4 (2 copies)
78-86 Commanding General, Second Army, Fort Meade, Md
ATTN: AIABB (1 copy)
AIABD (8 copies)
87-88 Commanding General, Third Army, Fort McPherson, Ga
ATTN: ACOFS G-3
89 Commanding General, Fourth Army, Fort Sam Houston, Tex
ATTN: G-3 Section
90 Commanding General, Fifth Army, 1660 E Hyde Park Blvd, Chicago 15, Ill
ATTN: ALFEN
91 Commanding General, Sixth Army, Presidio of San Francisco, Calif
ATTN: AMGCT-4
92-93 Commander-in-Chief, FECOM, APO 500, c/o PM, San Francisco, Calif
ATTN: ACOFS, J-3
94-96 Commanding General, US Army Forces Far East (Main), APO 343, c/o PM San Francisco, Calif
ATTN: ACOFS G-3
97 Commanding General, US Army Alaska APO 942, c/o PM, Seattle, Wn
98 Commanding General, US Army Carribean, Ft Amador, CZ
99 Commanding General, USARFANT & MDPR, Ft Brooke, PR
100-101 Commanding General, US Army Europe APO 403, c/o PM New York, NY
ATTN: OPOT Div, Combat Dev Br
102-103 Commanding General, US Army Pacific APO 958, c/o PM San Francisco, Calif
ATTN: Cmp Off
104 Commandant, Command & General Staff College, Ft Leavenworth, Kan
ATTN: ALLLS (AS)

INITIAL DISTRIBUTION (cont)

105 Commandant, The Infantry School, Ft Benning, Ga
ATTN: CDS
106 Commandant, The Artillery School, Ft Sill, Okla
107 Commandant, The AA&GM Branch, The Artillery School, Ft Bliss Tex
108-109 Commandant, The Armored School, Ft Knox, Ky
ATTN: Class Doc Sec, Eval & Res Div
110 Commanding General, Medical Field Service School, Brooke Army Medical Center, Ft Sam Houston, Tex
111 Director, Special Weapons Development Office, OCAFF, Ft Bliss, Tex
112 Commanding General, The Transportation Center & Ft Eustis, Ft Eustis, Va
ATTN: Asst Cmdnt, Mil Sci & Tactics Bd
113 The Superintendent, US Military Academy, West Point, NY
114 Commandant, Chemical Corps School, Chemical Corps Training Command, Ft McClellan, Ala
115 Commanding General, Research & Engineering Command, Army Chemical Center, Md
ATTN: Sp Proj Off
116-117 RD Control Officer, Aberdeen Proving Grounds, Md
ATTN: Dir, Ballistics Research Lab
118-120 Commanding General, The Engineer Center, Ft Belvoir, Va
ATTN: Asst Cmdnt, Eng School
121 Commanding Officer, Engineer Research & Development Lab, Ft Belvoir, Va
ATTN: Ch Tech Int Br
122 Commanding Officer, Picatinny Arsenal, Dover, NJ
ATTN: ORDBB-TK
123 Commanding Officer, Frankford Arsenal, Philadelphia 37, Pa
ATTN: RD Control Off
124-125 Commanding Officer, Chemical Corps Chemical & Rad Lab, Army Chemical Center, Md
ATTN: Tech Library
126 Commanding Officer, Transportation R&D Station, Ft Eustis, Va
127 Asst Chief, Military Plans Div, Rm 516, Bldg 7, Army Map Service, 6500 Brooks Lane, Washington 25, DC
ATTN: Operations Plans Branch
128 Director, Technical Documents Center, Evans Signal Lab, Belmar, NJ
129 Director, Waterways Experiment Station, PO Box 631, Vicksburg, Miss
ATTN: Library
130 Director, Operations Research Office, Johns Hopkins University, 6410 Connecticut Avenue, Chevy Chase, Md
ATTN: Library

NAVY

131-132 Chief of Naval Operations, D/N, Washington 25, DC
ATTN: Op-36

133 Chief of Naval Operations, D/N, Washington 25, DC
ATTN: Op-374
134-135 Chief, Bureau of Medicine & Surgery, D/N, Washington 25, DC
ATTN: Special Weapons Defense Division
136 Chief, Bureau of Ordnance, D/N, Washington 25, DC
137 Chief, Naval Personnel, D/N, Washington 25, DC
ATTN: Pers 112

INITIAL DISTRIBUTION (cont)

138 Chief, Bureau of Ships, D/N, Washington 25, DC
ATTN: Code 348
139 Chief, Bureau of Yards & Docks, D/N, Washington 25, DC
ATTN: P-312
140 Chief, Bureau of Supplies & Accounts, D/N, Washington 25, DC
141-142 Chief, Bureau of Aeronautics, D/N, Washington 25, DC
143 Chief of Naval Research, Code 219, Rm 1807, Bldg T-3, Washington 25, DC
ATTN: RD Control Off
144-147 Commandant, United States Marine Corps, Washington 25, DC
ATTN: Code A03H
148 President, US Naval War College, Newport, RI
149 Superintendent, US Naval Postgraduate School, Monterey, Calif
150-151 Commanding Officer, US Naval Schools Command, US Naval Station, Treasure Island, San Francisco, Calif
152-153 Director, USMC Development Center, USMC Schools, Quantico, Va
ATTN: Tactics Bd (1 copy)
Equipment Bd (1 copy)
154-155 Commanding Officer, US Fleet Training Center, Naval Station, San Diego 36, Calif
ATTN: SPWP School
156 Commanding Officer US Naval Damage Control Training Center, Naval Base, Philadelphia, Pa
ATTN: ABC Defense Course
157 Commanding Officer, US Naval Unit, Chemical Corps School, Army Chemical Tng Cntr, Ft McClellan, Ala
158 Joint Landing Force Board, Marine Barracks, Camp Lejeune, NC
159-161 Commander, US Naval Ordnance Laboratory, White Oak, Md, Silver Spring 19, Md
ATTN: EE (1 copy)
R (2 copies)
162 Commander, US Naval Ordnance Test Station, Inyokern, China Lake, Calif
163-164 Officer-in-Charge, US Naval Civil Engineering Research and Evaluation Lab, US Naval Construction Bn Center, Port Hueneme, Calif
ATTN: Code 753
165 Director, US Naval Research Laboratory, Washington 25, DC
166-167 Commanding Officer, US Naval Radiological Defense Laboratory, San Francisco 24, Calif
ATTN: Tech Info Div
168 Commanding Officer & Director, David W. Taylor Model Basin, Washington 7, DC
ATTN: Library
169 Commander, US Naval Air Development Center, Johnsville, Pa
170-171 Director, Office of Naval Research Branch Office, 100 Geary St, San Francisco 9, Calif

AIR FORCE

172 Asst for Atomic Energy, Hqs, USAF, Washington 25, DC
ATTN: DCS/O
173 Asst for Development Planning, Hqs, USAF, Washington 25, DC
174 Director of Operations, Hqs, USAF, Washington 25, DC
175 Director of Operations, Hqs, USAF, Washington 25, DC
ATTN: Operations Analysis
176 Director of Plans, Hqs, USAF, Washington 25, DC
ATTN: War Plans Div

INITIAL DISTRIBUTION (cont)

177 Director of Requirements, Hqs, USAF, Washington 25, DC
ATTN: AFDRQ-SA-M
178 Director of Research and Development, Hqs, USAF, Washington 25, DC
ATTN: Armament Div
179-180 Director of Intelligence, Hqs, USAF, Washington 25, DC
ATTN: AFOIN-1B2
181 The Surgeon General, Hqs, USAF, Washington 25, DC
ATTN: Bio Def Br, Pre Med Div
182 Commander, US Air Forces-Europe, APO 663, c/o PM NY, NY
183 Commander, Far East Air Forces, APO 925, c/o PM San Francisco, Calif
184-185 Commander, Alaskan Air Command, APO 942, c/o PM Seattle, Wn
ATTN: AAOTN
186 Commander, Northeast Air Command, APO 862, c/o PM NY, NY
187 Commander, Strategic Air Command, Offutt AFB, Omaha, Neb
ATTN: Chief, Operations Analysis
188 Commander, Tactical Air Command, Langley AFB, Va
ATTN: Doc Sec
189 Commander, Air Defense Command, Ent AFB, Colo
190-191 Commander, Air Materiel Command, Wright-Patterson AFB, Dayton, Ohio
ATTN: MCAIDS
192 Commander, Crew Training Air Force, Randolph AFB, Tex
ATTN: DCS/O 46TB
193-204 Commander, Flying Training Air Force, Waco, Tex
ATTN: Dir of Observer Tng
205 Commander, Hq. Technical Training Air Force, Gulfport, Miss
ATTN: TA&D
206 Commander, Air Training Command, Scott AFB, Belleville, Ill
ATTN: DCS/O GTP
207-209 Commander, Air Research and Development Command, PO Box 1395, Baltimore, Md
ATTN: RDDN
210 Commander, Air Proving Ground Command, Eglin AFB, Fla
ATTN: AG/TRB
211-212 Commander, Air University, Maxwell AFB, Ala
213-214 Commandant, Air Force School of Aviation Medicine, Randolph AFB, Tex
215-220 Commander, Wright Air Development Center, Wright-Patterson AFB, Dayton Ohio
ATTN: WCOESP
221 Commander, AF Cambridge Research Center, 230 Albany St, Cambridge 39, Mass
ATTN: CRTSL-2
222-224 Commander, Air Force Special Weapons Center, Kirtland AFB, New Mex
ATTN: Tech Library
225 Commandant, USAF Institute of Technology, Wright-Patterson AFB, Dayton, Ohio
ATTN: Resident College
226-227 Commander, Lowry AFB, Denver, Colo
ATTN: Dept of Armament
228-230 Commander, 1009th Special Weapons Squadron, Hqs, USAF, Washington 25, DC
231-232 The RAND Corporation, 1700 Main St, Santa Monica, Calif
ATTN: Nuclear Energy Div

AFSWP-460

INITIAL DISTRIBUTION (cont)

OTHER DOD ACTIVITIES

233 Executive Secretary, Joint Chiefs of Staff, Washington 25, DC
234 Director, Weapons Systems Evaluation Group, OSD, Rm2E1006, Pentagon, Washington 25, DC
235 Asst for Civil Defense, Office of Secretary of Defense, Washington 25, DC
236 Chairman, Armed Services Explosives Safety Board, DOD, Rm 2403, Barton Hall, Washington 25, DC
237 Asst Secretary of Defense, Research and Development, Washington 25, DC
ATTN: Tech Library
238 Executive Secretary, Military Liaison Committee, PO Box 1814, Washington 25, DC
239 Commandant, National War College, Washington 25, DC
ATTN: Classified Records, Library
240 Commandant, Armed Forces Staff College, Norfolk 11, Va
ATTN: Secretary
241-246 Commanding General, Field Command, AFSWP, PO Box 5100, Albuquerque, New Mex
247-266 Chief, Armed Forces Special Weapons Project, PO Box 2610, Washington 13, DC

~~CONFIDENTIAL~~ UNCLASSIFIED

14617

DEPARTMENT OF DEFENSE
ARMED FORCES SPECIAL WEAPONS PROJECT
P. O. BOX 2610
Washington 13, D. C.

SWPEF-4 461.1 13 January 1954

SUBJECT: Transmittal of Report - AFSWP-460

TO: Distribution List

Transmitted herewith, for your information and permanent retention, (is) (are)(copy)(copies) of AFSWP-460 as indicated on Inclosure #1.

FOR THE CHIEF, AFSWP:

H. H. Rankin

H. H. RANKIN
Lt. Colonel, AGC
Adjutant General

2 Incls:
1. Receipt (dup)
2. As stated above

WHEN SEPARATED FROM INCLOSURES HANDLE
THIS DOCUMENT AS - UNCLASSIFIED -

~~CONFIDENTIAL~~ ~~RESTRICTED DATA~~
~~ATOMIC ENERGY ACT 1946~~

UNCLASSIFIED

UNCLASSIFIED

CONFIDENTIAL SECURITY INFORMATION

CONFIDENTIAL SECURITY INFORMATION

UNCLASSIFIED